Towards A Parallel Wireless Radio Communication Architecture for Modular Robots

Victor Kuo and Robert Fitch
ARC Centre of Excellence for Autonomous Systems
Australian Centre for Field Robotics (ACFR)
The University of Sydney, NSW Australia
{v.kuo, rfitch}@acfr.usyd.edu.au

Abstract

Provisioning a scalable communication architecture in self-reconfiguring (SR) modular robots is one of the major challenges in their large-scale implementation in hardware. The infrared and hardwired communication systems usually employed are complex, are unreliable, and can lead to unrecoverable errors. Wireless mesh networks offer a robust and versatile solution but do not scale in terms of bandwidth and latency. By exploiting the unique properties of modular robots, we address the *scalability problem* in this paper. We propose a novel multi-radio, multi-channel mesh network architecture that guarantees fixed bandwidth and latency for inter-module communication, independent of the robot size. We present experimental results using modified ZigBee radios in a well-controlled setup that is free from unpredictable properties of radio propagation such as multi-path interference. By eliminating variables that would otherwise be present in a practical environment, we are able to precisely validate the principles and assumptions of our architecture. Using results from our experiments as a baseline we also qualitatively show that our approach has in-built protection from multi-path interference.

1 Introduction

Self-reconfiguring (SR) modular robots are decentralised systems that fundamentally rely on inter-module communication in performing basic tasks such as locomotion and reconfiguration planning. The provisioning of a scalable and robust communication architecture is one of the major challenges that still exist in the practical implementation of these systems [Yim *et al.*, 2007a]. Most SR robots use hardwired [Kurokawa *et al.*, 2007; Yim *et al.*, 2000] and/or infrared (IR) connections [Gilpin *et al.*, 2008; Salemi *et al.*, 2006; Castano *et al.*, 2002; Jorgensen *et al.*, 2004; Yim *et al.*, 2007b] which are designed into the module surfaces. Consequently the communication model is conventionally assumed to be point-to-point as illustrated in Fig. 1. Hardwired solutions, whilst offering unparalleled bandwidth, require complex connector designs. They also require accurate alignment and orientation between two connecting modules. IR only requires approximate alignment of beams but suffers from cross talk and is unreliable in outdoor conditions where dust and dirt can abrade or obstruct the optics. Failure of a connection-dependent communication system can lead to unrecoverable module failure in cases where a given module is attached by only a single connector.

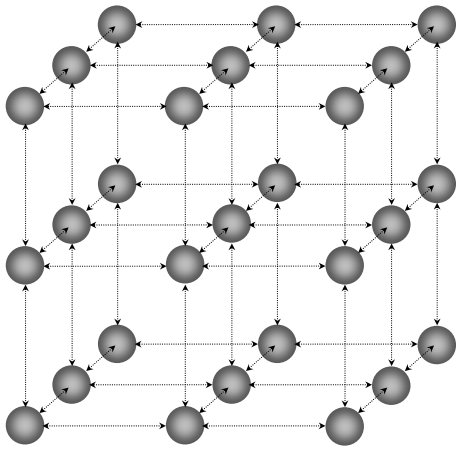

Figure 1: A three-dimensional lattice of modules with arrows indicating traffic characteristics typical of modular robots. Point-to-point communication in lattice space is assumed.

Radio frequency (RF) radios, on the other hand, are free from the above problems. RF radios also provide advantages such as non line-of-sight wireless communication between modules, which is necessary for inter-

cluster reconfiguration manoeuvres. RF radios are also more versatile. Unlike IR and hardwired systems, an RF system can be installed in any modular robot without regard to the inter-module docking orientation and mechanism.

In SR robots, the most practical way of implementing inter-module communication with radios is to deploy a mesh network. A mesh network is a collection of interconnected radio nodes (modules). This differs from traditional wireless networks such as wireless access points which have a central coordinating node in a star topology. A mesh network has a distributed flat topology with no coordinator and each node can connect to multiple neighbours as seen in Fig. 1.

Mesh networks however have one critical shortfall: bandwidth and latency scalability. In a seminal paper by Gupta and Kumar [Gupta and Kumar, 2000] it was shown that the capacity of mesh networks scales by $\theta(\sqrt{n})$ as the number of nodes n grows to infinity. This implies that the bandwidth available to each node scales by $\theta(\sqrt{\frac{1}{n}})$ and hence mesh networks are not suitable for applications with large numbers of nodes. Subsequent to this result, Li et al. [Li *et al.*, 2001] identified that there are assumptions made in [Gupta and Kumar, 2000] which do not apply in certain mesh network applications. The removal of such assumptions has positive implications on scalability. Three assumptions made that are contrary to the interest of SR robots include:

1. The likelihood that any pair of nodes are communicating is equal for all nodes in the network.
2. Each node has only one radio and the network operates on a single channel.
3. Nodes are randomly located.

The first assumption is the fundamental reason that bandwidth capacity in mesh networks does not scale. In SR robotics, however, nodes communicate only with their immediate neighbours and global communication is not necessary (see Fig. 1). The second assumption is the main cause of unacceptable latency in large mesh networks. However by using multiple radios operating on orthogonal channels in a single node (multi-radio multi-channel node), combined with the removal of the first assumption, scalability becomes independent of n. As for the third assumption, nodes in SR robots are typically located at regular intervals and often in a lattice structure as seen in Fig. 1. Trivial prior to the removal of the first two assumptions, the third assumption allows us to place guarantees on bandwidth and latency as well as efficient allocation of channels to the multi-radio multi-channel (MRMC) mesh network. Hence we see that under the right assumptions, mesh networks are indeed scalable in bandwidth and latency.

In this paper we propose a new MRMC mesh network architecture that exploits these unique properties of modular robots to address the scalability problem. Through channel reuse our architecture guarantees a minimum bandwidth and latency for inter-module communication that is independent of the network size and applicable to two and three-dimensional networks. We present experiments with ZigBee radios that validate our assumptions and successfully show proof-of-concept for the presented network architecture. We also qualitatively analyse the performance of our system in practical environment focusing on the impact of multi-path interference which cannot be simulated in a controlled experimental environment.

2 Related Work

Most SR robots use hardwired or IR for communication. See [Fitch and Lal, 2009] for details. There already exist several modular robot implementations that use wireless communication including [Moeckel *et al.*, 2006; Yim *et al.*, 2007b; Kurokawa *et al.*, 2007; An, 2008; Detweiler *et al.*, 2007; Gilpin *et al.*, 2008]. The majority of these robots use wireless radios in a star topology for user control purposes and not inter-module communication.

In [An, 2008], off-the-shelf ZigBee modules are used for inter-module communication. The paper demonstrates a small, 8-module system where scalability is not a concern.

Thus far the most extensive use of RF wireless mesh networks for communication is in the *YaMor* robot[Moeckel *et al.*, 2006], which successfully incorporates a Bluetooth Scatternet. Bluetooth uses Frequency Hopping Spread Spectrum (FHSS) and has a master-slave architecture which makes it cumbersome to deploy Bluetooth in a mesh network topology (as evidenced by the need for a custom Scatternet protocol). This approach guarantees low latency, but the bandwidth scalability will still be an issue as the number of modules approaches the number of orthogonal channels (79) available.

The use of ZigBee radios for SR robots was evaluated in experiments involving 15 ZigBee modules in [Fitch and Lal, 2009]. The results indicated that the use of ZigBee wireless radios is feasible as a simple low-cost communication system, however scalability still remains a problem.

There is an immense body of work from the communication community on developing efficient and scalable architectures and protocols for mesh networks [Akyildiz and Wang, 2005]. However to the best of our knowledge this is the first paper to specifically address the scalability problem of mesh networks in modular robots. The closest system with similar communication characteristics to SR robots is the cellular network. Mobile phone

networks, however, use a hierarchal architecture serviced by a hardwired backbone. Modular robotics cannot rely on such infrastructure and must use a distributed architecture.

3 Architecture Overview

Our proposed parallel wireless communication system is based on an MRMC mesh network architecture. Fig. 2 depicts one possible layout in which robot modules are placed in a two-dimensional square lattice. Each module will have at least two radios. One radio will be allocated a fixed channel that is unique amongst its neighbours and all incoming data to the module will be received through this radio. We shall refer to this as the home channel of the module. The second radio is used to transmit data to neighbouring modules and will rapidly switch channels to match the home channel of its neighbours. To prevent collisions with other neighbouring modules with the same recipient, the home radio of every module operates a Time Division Multiple Access (TDMA) scheme. TDMA is a channel access method used by wireless radios for dividing bandwidth on a channel into time slots which can be allocated to specific users [Rappaport, 2001]. Additional radios can also be added for transmission if channel switching causes too much delay or if concurrent transmission to multiple neighbours is a necessary feature. In our design we have chosen to use IEEE 802.15.4 compliant transceivers. Given that the typical unit purchase price these front end radios is approximately 3-5USD (in 2009) the use of multiple radios is still cost effective. Our radio hardware choice is explained in further detail in Sec. 4.1.

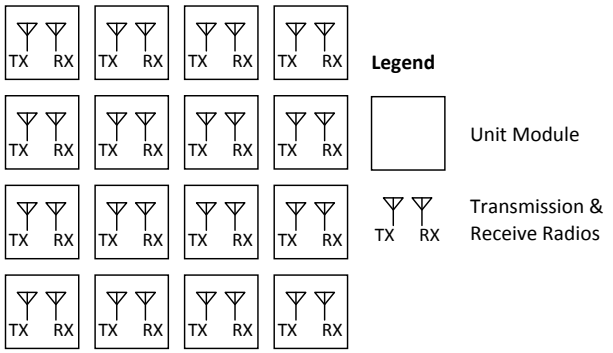

Figure 2: A multi-radio multi-channel network for a modular robot lattice layout.

If there were enough orthogonal channels to allocate each module a unique home channel, our solution would be complete. Each module is guaranteed immediate access to all bandwidth on its home channel. However SR robots are envisioned to contain hundreds or thousands of individual modules and there is a finite number of orthogonal channels available. We now face the question of whether there are enough orthogonal channels available to allocate to modules within an area such that the same orthogonal channels can be reused elsewhere without causing co-channel interference. We assume that Carrier Sense Multiple Access (CSMA) is not been used and that all modules are constantly communicating with their neighbours so an opportunistic on-demand channel allocation scheme is not feasible. CSMA is a channel access scheme where the transmitting radio will check that the channel is idle before broadcasting so that the signals are not corrupted [Stallings, 1997]. Instead our design will use a fixed channel allocation scheme where channels are reused at regular intervals.

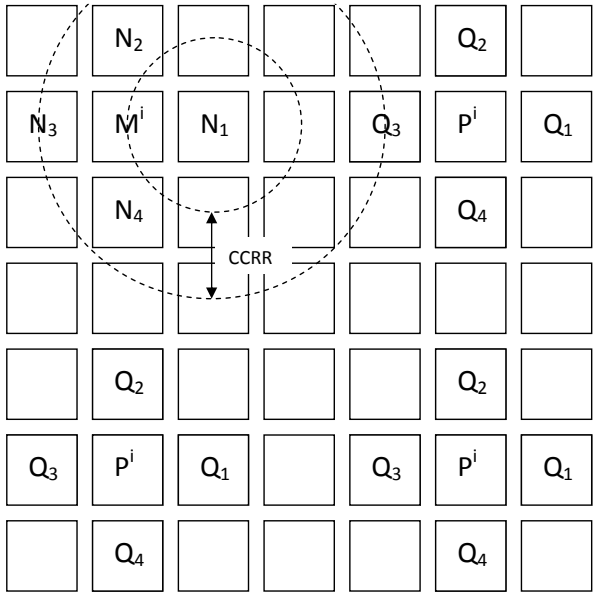

Figure 3: Calculating minimum number of orthogonal channels and interference range.

We illustrate the channel allocation problem in Fig. 3. Let module M be allocated channel i such that its immediate neighbours N_i communicate to M on channel i. If another module P is also allocated channel i, how far must it be from M such that the signal from any of P's neighbours Q_i is stronger than the signal from any N_i module by SdB where S represents the co-channel rejection ratio (CCRR) of the radio? This problem is answered by applying the free-space path loss (FSPL) equation to convert the CCRR from decibels to Euclidean distance which we shall refer to as the *interference range* of the radio. If the Euclidean interference range $d_{interference_range}$, represents the necessary separation between two radios for interference-free channel

reuse then we have

$$d_{interference_range} = 10^{\frac{CCRR+20\log_{10}(D_{neighbour_distance})}{20}} \quad (1)$$

where $CCRR$ is the co-channel rejection ratio in dB and determined by the radio hardware specifications and $D_{neighbour_distance}$ is the maximum Euclidean distance from the receive antenna in one module to the transmit antenna of the neighbouring radio.

CCRR is similar to the more commonly used *Signal to Noise Ratio (SNR)*. It quantifies the necessary signal strength ratio between a desired and interfering signal such that the desired signal can be correctly received without corruption. The FSPL equation describes the rate at which an electromagnetic wave attenuates in free space [Rappaport, 2001].

After determining the Euclidean interference range of a transmitting radio we can apply Brooks's $\triangle$-colouring algorithm [Brooks, 1941] on the resulting interference graph. This determines the minimum number of orthogonal channels required to reuse frequencies without causing co-channel interference.

We illustrate the entire process of calculating the interference range and minimum orthogonal channels in an example based on Fig. 3. First we draw two circles around each neighbour of module M which is done for N_1 in Fig. 3. The inner circle has a radius equal to the maximum distance from the transmit antenna in the neighbour module N_i to the receive antenna in the master module M. The outer circle is drawn with a radius such that the signal attenuation from the inner circle to the outer circle is greater than the CCRR required by the radio hardware. The sum of the number of modules encompassed by the outer circle of all neighbours N_i of M is the number of orthogonal channels required for interference-free channel reuse. The outer circle is also the channel reuse separation required for interference-free channel reuse.

3.1 Three-Dimensional Networks

Thus far we have assumed only a two-dimensional network, however this method for calculating the minimum orthogonal channels and interference range can also be applied in three-dimensional lattices. In calculating the three-dimensional case, circles are simply replaced with spheres or whichever volume best represents the gain pattern of the antenna used. Our architecture scales to a three-dimensional lattice without any modification in terms of hardware or software other than the need for a larger number of orthogonal channels. An alternative to using more orthogonal channels would be to used a radio hardware which supports Code Division Multiple Access (CDMA) which is the approach used in mobile phone networks [Rappaport, 2001]. In the case of using CDMA, each code division acts as an orthogonal channel hence artificially increasing the number of non-interfering channels of communication.

4 Experiment Setup

In this section we discuss the hardware and software that was used in the experiments to show proof-of-concept. We also discuss the precautions that were taken to ensure accurate and reproducible results.

4.1 Hardware Selection

In selecting the hardware, we considered the following criteria:

1. Radios must support multiple orthogonal channels.
2. A high CCRR is preferable (-6dBm or more).
3. Radios can operate without using CSMA.

Based on the above criteria, IEEE 802.15.4 and ZigBee standard radios were used for the experiments. IEEE 802.15.4 operates in the unlicensed RF spectrum of 868, 915 and 2400MHz with respective data rates of 20, 40 and 250kbps. In our experiment, 2400MHz radios were selected for the higher data rate and because the 2400MHz radios have 16 orthogonal channels as oppose to only 10 in the 915MHz band and 1 in the 868MHz band.

The IEEE 802.15.4 standard also includes the capacity for a TDMA scheme which does not use CSMA. The ability to operate the radios without CSMA is critically important as a single radio can easily transmit a signal strong enough to force all modules in the SR robot to back-off in the CSMA algorithm.

Other radio standards such as Bluetooth (IEEE 802.15.1) were also considered. Bluetooth has advantages such as a higher data rate (1Mbps) and 79 orthogonal channels. However the IEEE 802.15.1 standard gives limited control over the channels which the Frequency Hopping Spread Spectrum (FHSS) scheme hops over making it difficult to efficiently utilise the larger number of orthogonal channels. The master-slave architecture in Bluetooth also adds to the complexity of the design as the transmit radios in our architecture would have to form Scatternets with their master and rapidly switch between the Piconets.

IEEE 802.11a radios were also considered however they consume more power and are more expensive, making them unsuitable for a battery operated MRMC architecture. IEEE 802.11b/g radios also only have 3 orthogonal channels.

4.2 Hardware Implementation

Jennic JN5139 2.4GHz ZigBee modules [Jennic, 2009] were chosen to conduct the experiments. The module includes a 32-bit CPU, 96kB of RAM, 192kB of flash

memory and chip antenna. These modules are more expensive (around 20USD in 2008) than purchasing front end radio transceivers. However the onboard processing and memory provided significant time savings in hardware design and construction which is more appropriate for a proof-of-concept test. The modules were also slightly modified by removing the chip antennas to dramatically reduce the transmission strength as shown in Fig. 4. This was a necessary step to negate the effects of multi-path fading which would have otherwise made it extremely difficult to make accurate and repeatable measurements of signal strength with small changes in distance. The removal of the antenna effectively reduced the transmission range to approximately 20-30cm.

4.3 Software

The testing software is implemented on the IEEE 802.15.4 stack. Each radio is setup either as a network coordinator or an end device to simulate the receive and transmit radio in the modules respectively. The purpose of the software is to measure throughput between a master-neighbour pair of radios when subjected to varying amounts of interference.

The network coordinator (master radio) on startup begins a beacon-enabled network with a beacon order and superframe order of 8 (see [IEEE Std 802.15.4, 2003] for details) and then waits for the end device (neighbour module) to join. Each end device on power up begins listening for network coordinator beacons. Once the end device hears a beacon, it sends an association request to join the network. Once the end device has successfully joined to the coordinator network, it requests for all 15 of the available transmission slots called Guaranteed Time Slots (GTS) as described in [IEEE Std 802.15.4, 2003]. After the GTS has been allocated by the coordinator, the end device begins transmitting at the full data rate without applying the CSMA algorithm during transmission. To measure the throughput, the coordinator records the number of bytes received per unit time to calculate the throughput data rate. This information as well as the signal strength of each received packet, is printed through a serial port to a monitoring computer. The throughput data rate at the coordinator is then used as a test for the presence of interference. Fig. 5 illustrates the process described above.

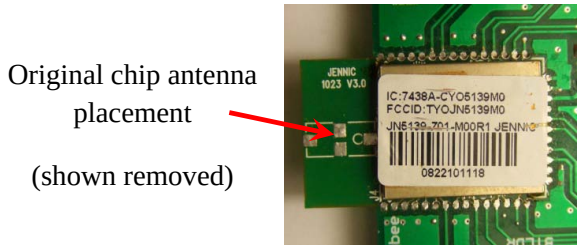

Figure 4: Jennic ZigBee module with chip antenna removed.

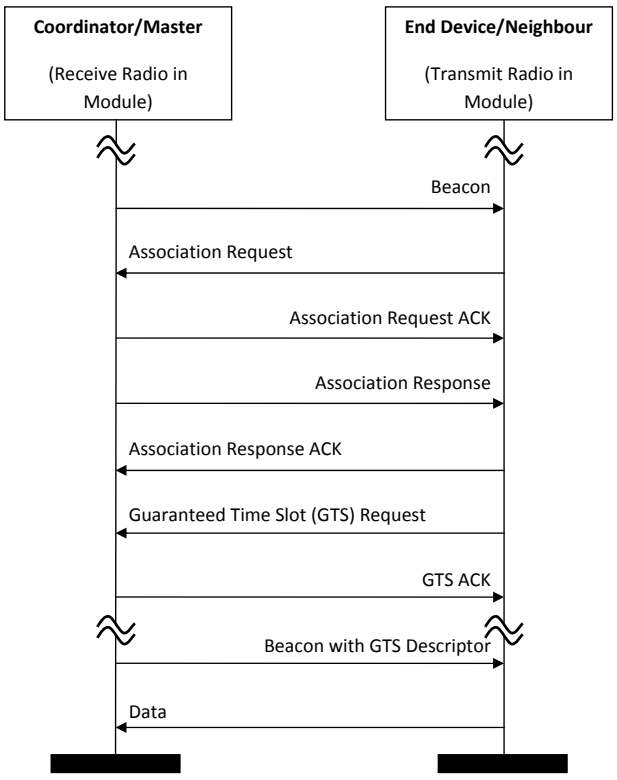

Figure 5: Software message sequence chart.

4.4 Testbed

In an effort to create accurate and reproducible results, a significant amount of consideration was given to how the testbed should be configured. To make the testbed realistic we should test the radio architecture in a representative modular robot to model the operational environment. However it is well known that wireless experiments are notoriously difficult to reproduce due to the unpredictable nature of radio propagation [De *et al.*, 2005] and the effects of multi-path interference. Part of any well designed and executed experimental procedure is to first establish a reproducible baseline to validate the fundamental theories and predictions that have been put forward. Whilst this may add to the development time of a project, moving straight to a realistic testbed would inject too many variables into the experiment.

For this reason we decided to test the architecture in controlled environment in order to establish a firm foundation on which future experiments can be conducted. Our testbed is set up in an open-space environment where the radio modules are elevated off the ground on stands as seen in Fig. 6 to minimise signals reflecting off

the floor and other multi-path effects. The stands and platforms are made from wood and foam respectively to further reduce the effect of the setup on the radio signal propagation. The radios are placed in an open room with at least one metre of clearance on all sides of the radios. This clearance is which is sufficient to eliminate reflections off walls since the maximum transmission range is only approximately 20-30cm with the removal of the chip antenna. Whilst these conditions are ideal and far removed from the real environment, when we do extend our work to a real modular robot we will be in a much stronger position to establish and address new problems.

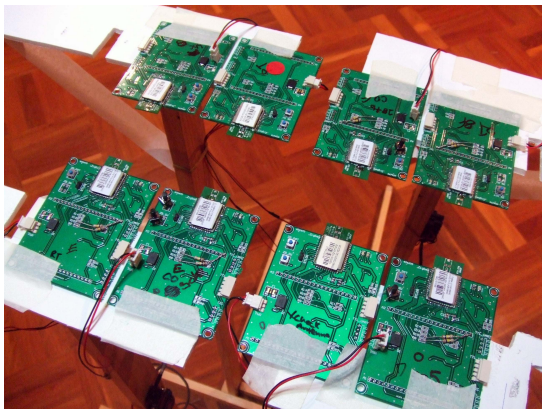

Figure 6: Proof-of-concept experiment setup with four pairs of radios.

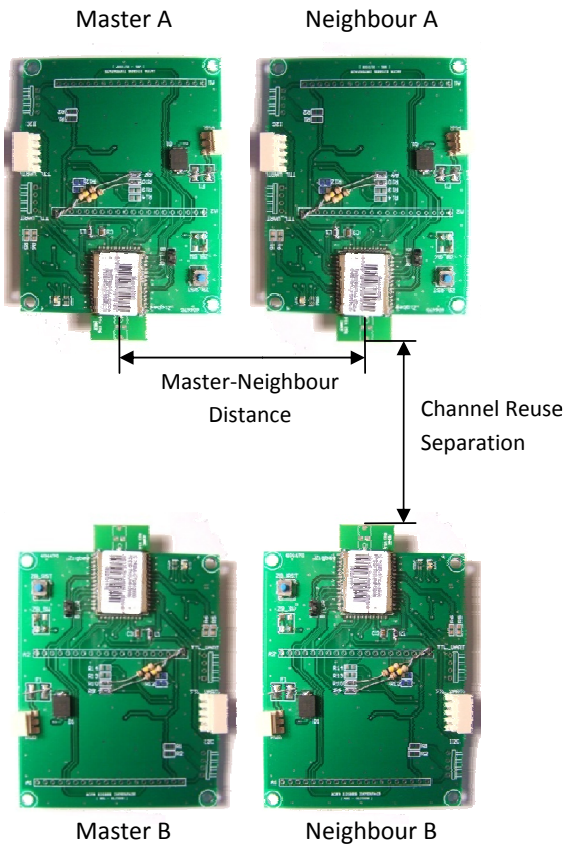

Figure 7: Setup for measuring signal attenuation and co-channel rejection ratio.

5 Experiments and Results

In this section we present experimental proof-of-concept for our proposed MRMC architecture. We demonstrate pairs of radios (simulating neighbour-to-neighbour communication) in a tiled manner as seen in Fig. 3. Each pair is able to communicate without interference from neighbouring pairs operating on the same channel. To avoid confusion, from here on we shall refer to a transmitting neighbour and a receiving neighbour as a *master* and a *neighbour*, respectively. For example in Fig. 3, module M^i is a master and modules N_i are neighbours of M^i (note all modules are also masters of their neighbours).

We performed three experiments: 1) we measured attenuation characteristics of the radios to verify the FSPL decay in signal strength; 2) we then determined the CCRR of the radios for successful co-channel operation; and 3) we demonstrated the operation of four pairs of radios operating on the same channel simultaneously and without interference to simulate channel reuse. Whilst the first two tests seem trivial to characterise accurately through equations and data sheets, it is widely accepted that theoretical and practical characteristics of radios can differ immensely [Kotz *et al.*, 2003].

5.1 Attenuation Measurements

To measure the attenuation characteristics of our radio hardware we used the setup shown in Fig. 7. The signal attenuation is measured using the software in Sec. 4.3 by recording the average signal strength of each received packet at varying distances. The results presented in Fig. 8 shows the relationship between signal strength in dBm versus the separation distance between the antenna of the two radios. Different radio orientations are also measured. The *Frontward Orientation* curve corresponds to varying the Master A Master B distance and the *Sideward Orientation* curve represents varying the Master A Neighbour B distance in Fig. 7. The third curve represents the theoretical FSPL at 2.4GHz.

It is apparent from Fig. 8 that the attenuation characteristics differ from the theoretical FSPL curve and also differ depending on the orientation of the radios. The most likely explanation for the deviation from the theoretical inverse square attenuation is the non-linearity of the hardware gain amplifiers in the radios and the layout of the dielectric circuit board. However the deviation is not significant enough to be of concern.

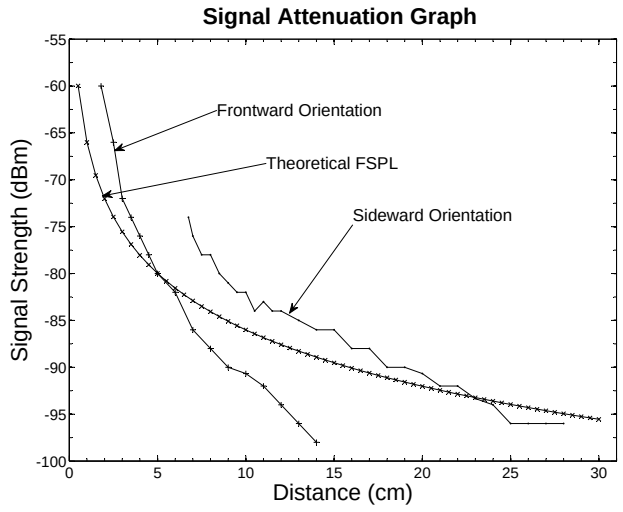

Figure 8: Radio signal attenuation graph.

5.2 Co-Channel Rejection Ratio Measurement

To measure the CCRR of the radio hardware, two pairs of radios are setup as seen in Fig. 7. Both pairs of radios are set to the same channel and assigned unique network identifiers. Using the software in Sec. 4.3 we begin by verifying that each master-neighbour pair of radios is communicating at the full data rate possible (183kbps) in the absence of interference.

For various *Master-Neighbour Distances* as shown in Fig. 7 we determine the *Channel Reuse Separation* (Euclidean separation between two master-neighbour pairs) necessary for interference-free transmission and then convert this Euclidean distance to dBm using the Frontward Orientation curve in Fig. 8.

The minimum Channel Reuse Separation is determined by slowly bringing together the two pairs of radios and recording the data rate at different distances. The results shown in Fig. 9 illustrates three curves representing a Master-Neighbour Distance of 3, 7 and 10cm with a respective signal strength of -84, -78 and -48dBm.

For each of the three Master-Neighbour Distances the graphs clearly show a sharp transition from the full baseline data rate of 183kbps to 0kbps. The transition occurs at -66, -80 and -86dBm for *Master-Neighbour Signal Strengths* of -84, -78 and -48dBm respectively. By subtracting the signal strength at the transition point from the Master-Neighbour Signal Strength of the curve we can determine CCRR's of -2, -2 and -4dBm respectively. According to the JN5139 data sheet, the signal amplifier has 47 gain stages and each one is approximately 2dBm which explains the sharp transition from full data rate to zero throughput.

Assuming a -2dBm CCRR and applying Equation 1 we determine that the minimum channel reuse separation required is 1.25 times the master-neighbour distance. Since modules can only be placed at fixed intervals, the minimum separation is twice the master-neighbour distance. This thus proves that the topology and channel reuse separation as depicted in Fig. 3 is more than sufficient for interference-free channel re-allocation. In fact, after applying Brooks's $\triangle$-colouring algorithm we find that 13 orthogonal channels are sufficient for implementing our architecture on a two-dimensional lattice and 25 channels are necessary for a three-dimensional lattice.

5.3 Proof-of-Concept Demonstration

In this final proof-of-concept demonstration, the radios are physically setup as shown in Fig. 6. Each stand contains one master and one neighbour radio. Each of the four pairs of radios are separated by at most 1.25 times the master-neighbour distance as calculated in Sec. 5.2. All radios are set to the same channel and each master-neighbour pair is assigned a unique network identifier. Using the three Master-Neighbour Distances tested in Sec. 5.2 we were successful in making all four master-neighbour pairs communicate without interference at the full base-line data rate, on the same channel and separated by distances calculated in Equation 1 (1.25 times the master-neighbour distance). Each test was allowed to run for 30 minutes to ensure that the results were reliable and throughput was consistent. The fact that all four pairs operated without co-channel interference shows that compact channel reuse is achievable and proves that our architecture is feasible.

6 Interference at Larger Scale

Interference is a real issue in radio communication and is unavoidable and unpredictable in a real environment. For this reason it is difficult to *quantitatively* characterise the effects of interference without actually performing the experiments in the real environment. However it is possible to *qualitatively* analyse the impact of interference to predict the likely performance of the system. There are two types of interference that we must account for. First is interference from external sources in the same frequency band such as 802.11 transmitters or Zigbee radios. Secondly multi-path fading causing local areas of constructive destructive interference.

6.1 External Interference

The proliferation of radio transmitters in the 2.4Ghz spectrum makes external interference a concern for all transceivers in this band. Fortunately external interference poses less of a problem in our architecture as our radios are operating at extremely close distances and have very strong signal strengths. In fact we had to deliberately remove the antennas to reduce the signal strength

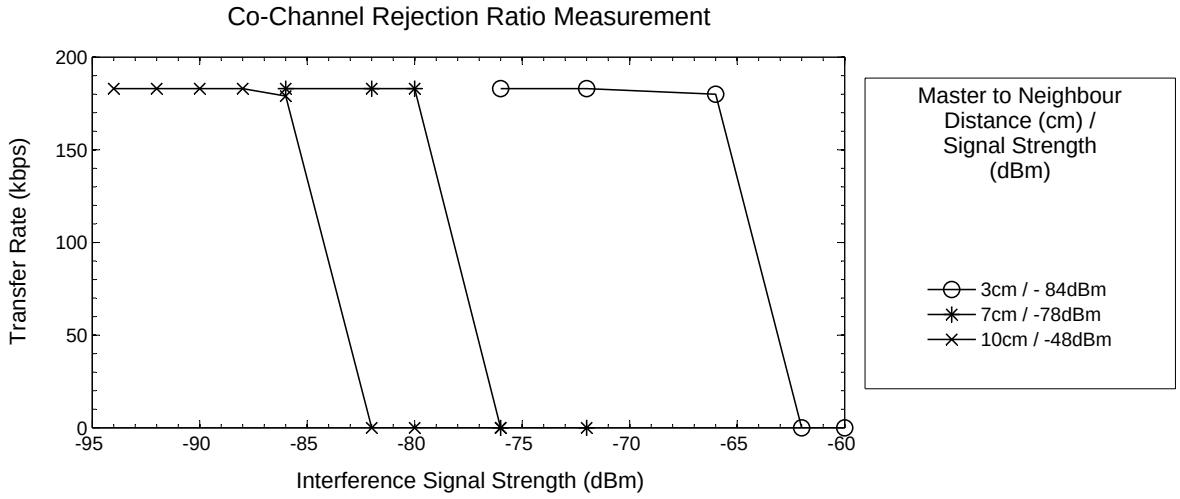

Figure 9: Results for co-channel rejection ratio measurements.

and prevent the amplifiers from saturating. Hence if there were any external signals strong enough to interfere with our system then all other radios in the spectrum will also be affected.

6.2 Multi-path Interference

Multi-path fading is a radio propagation phenomenon in which radio signals radiating from a single point source take different paths to the receiver due to reflections off obstacles in the environment. As the distance traversed from transmitter to receiver varies depending on the path traversed, the receiver radio sees the same signal arriving at different times with slight phase shifts which can cause constructive and destructive interference at the receiver. In a practical implementation multi-path fading can result from signals reflecting off the materials that make up the modules themselves and from signal reflections from obstacles external to the robot as it moves through the environment. The mobile nature of modular robots also means that interference occurs in an unpredictable manner and the architecture must be able to compensate for this.

Constructive multi-path interference can cause interference at a distant module reusing the same channel. In this case the interfering signal at a module is greater than the desired signal from the module's neighbours. Firstly we analyse the amount of constructive multi-path interference is necessary to corrupt the wanted signal to quantify the impact of constructive multi-path interference.

By examining the channel tiling pattern illustrated in Fig. 3 we can determine the minimum amount of constructive multi-path interference necessary to cause signal degradation. This is found by looking at radio M^i in Fig. 3 and finding the closest radio reusing the same channel which is Q_3. By using the signal strength of M^i's neighbours ($N_1 \sim N_4$) as the reference level of 0dB, then Q_3's signal is only -9.5dB in strength. Given that our radios have a CCRR of 2dB then Q_3 must be 7.5dB stronger than the line-of-sight signal to cause interference. In the same manner as above the signal of Q_2/Q_4 and Q_1 needs to be 10.3dB and 11dB respectively to cause interference. In our analysis we do not consider the effects of interference on transmitting neighbour radios ($N_1 \sim N_4$) as traffic flows from neighbour to master and the only transmissions from masters to neighbours are small acknowledgement packets which are optional. To generate the levels of interference stated above using Rayleigh fading, which is a widely accepted model for multi-path fading in non-line-of-sight situations, the likelihood of constructive interference with a magnitude of greater than 7.5dB is very low. The multi-radio architecture also puts our system in a strong position to further improve immunity to multi-path interference by using antenna diversity techniques. Assuming that both radios in a module are controlled by a single processor we can simply switch the master and transmit radios such that the position of both radios relative to its neighbours move by a fraction of a wavelength. This is a common technique used in many wireless base stations. Alternatively each radio can have multiple antennas either in microstrip or whip form and switch antennas using an RF switch. Hence on the detection of unacceptable amounts of interference, the master and transmit radios switch roles.

A common feature of multi-path fading is local points of extremely low signal strength called deep fades. This phenomenon would also impact on neighbour to master

transmissions. In the case of radios M^i and N_1, a deep fade could mean that the signal N_1 to M^i is lower by 7.5dB and hence signals from co-channel radio Q_3 interfere with its transmissions. Since deep fades are more common and can be as low as -40dB, antenna diversity techniques offer the best protection.

The unpredictable nature of multi-path propagation makes it difficult to accurately characterise without performing a full scale implementation which is not feasible for a proof-of-concept experiment. However despite the difficulties in quantitatively determining the impact of interference on our architecture, a qualitatively analysis shows that overall our architecture can be made resilient to external interference and multi-path effects using simple and existing techniques.

7 Conclusions and Future Work

Our experimental results demonstrate that compact channel reuse is achievable with off-the-shelf ZigBee radios. We successfully demonstrated four pairs of radios operating without interference on the same channel which validates the feasibility of our architecture design with existing hardware. We also qualitatively analysed the multi-path interference issues associated with migrating to a scaled hardware implementation and showed that constructive and destructive multi-path interference can be countered with simple and commonly used techniques. We conclude that our architecture can guarantee bandwidth and latency independent of the number of modules in the robot.

We are encouraged by our positive experiment results and plan to design and implement actual modules with an MRMC communication architecture. This will allow us to test our proposed design in a setup that is more representative of a modular robot.

The proposed communication architecture can also have applications in the wider distributed robotics community as well as in systems requiring scalable mesh networks. In fact any mesh network in which communication amongst nodes is purely local can potentially benefit from this network architecture.

Acknowledgments

This work is supported by the Australian Research Council (ARC) Centre of Excellence programme, funded by the ARC and the New South Wales (NSW) State Government. We would like to thank Ritesh Lal for the support he provided with the radio hardware. We would also like to thank Prof. Gregory J. Pottie for useful discussions and insightful advice.

References

[Akyildiz and Wang, 2005] I. Akyildiz and X. Wang. A survey on wireless mesh networks. *IEEE Comm. Mag.*, 43(9):S23–S30, 2005.

[An, 2008] B.-K. An. Em-cube: cube-shaped, self-reconfigurable robots sliding on structure surfaces. In *Proc. of IEEE ICRA*, pages 3149–3155, 2008.

[Brooks, 1941] R. Brooks. On colouring nodes of a network. *Proc. of Cambridge Philos. Soc.*, 37:194–197, 1941.

[Castano *et al.*, 2002] A. Castano, A. Behar, and P. Will. The CONRO modules for reconfigurable robots. *IEEE Trans. on Mechatronics*, 7(4):403–409, Dec. 2002.

[De *et al.*, 2005] P. De, A. Raniwala, S. Sharma, and T.-C. Chiueh. Design considerations for a multihop wireless network testbed. *Communications Magazine, IEEE*, 43(10):102–109, Oct. 2005.

[Detweiler *et al.*, 2007] C. Detweiler, M. Vona, Y. Yoon, S.-K. Yun, and D. Rus. Self-assembling mobile linkages. *IEEE Robot. Automat. Mag.*, 14(4):45–55, Dec. 2007.

[Fitch and Lal, 2009] R. Fitch and R. Lal. Experiments with a ZigBee wireless communication system for self-reconfiguring modular robots. In *Proc. of IEEE ICRA*, pages 1947–1952, 2009.

[Gilpin *et al.*, 2008] K. Gilpin, K. Kotay, D. Rus, and I. Vasilescu. Miche: Modular shape formation by self-disassembly. *Int. J. Rob. Res.*, 27(3-4):345–372, 2008.

[Gupta and Kumar, 2000] P. Gupta and P. Kumar. The capacity of wireless networks. *IEEE Trans. on Information Theory*, 46(2):388–404, Mar 2000.

[IEEE Std 802.15.4, 2003] IEEE Std 802.15.4. IEEE Standard for Part 15.4: Wireless Medium Access Control (MAC) and Physical Layer (PHY) Specifications for Low-Rate Wireless Personal Area Networks (LR-WPANs). *IEEE Std 802.15.4-2003*, pages 1–670, 2003.

[Jennic, 2009] Jennic. `http://www.jennic.com/`. Web-Site, September 2009.

[Jorgensen *et al.*, 2004] M. Jorgensen, E. Ostergaard, and H. Lund. Modular ATRON: modules for a self-reconfigurable robot. In *Proc. of IEEE IROS*, pages 2068–2073, 2004.

[Kotz *et al.*, 2003] D. Kotz, C. Newport, and C. Elliott. The mistaken axioms of wireless-network research. Technical Report TR2003-467, Dartmouth College, Computer Science, July 2003.

[Kurokawa *et al.*, 2007] H. Kurokawa, K. Tomita, A. Kamimura, S. Kokaji, T. Hasuo, and S. Murata. Self-reconfigurable modular robot M-TRAN: distributed control and communication. In *Proc. of RoboComm*, pages 1–7, 2007.

[Li *et al.*, 2001] J. Li, C. Blake, D. De Couto, H.-I. Lee, and R. Morris. Capacity of ad hoc wireless networks. In *Proc. of MobiCom*, pages 61–69, 2001.

[Moeckel *et al.*, 2006] R. Moeckel, C. Jaquier, K. Drapel, E. Dittrich A. Upegui, and A.-J Ijspeert. Exploring adaptive locomotion with YaMoR, a novel autonomous modular robot with bluetooth interface. *Industrial Robot: An International Journal*, 33:285 – 290, 2006.

[Rappaport, 2001] T. Rappaport. *Wireless Communications: Principles and Practice*. Prentice Hall PTR, Upper Saddle River, NJ, USA, 2001.

[Salemi *et al.*, 2006] B. Salemi, M. Moll, and W.-M. Shen. Superbot: A deployable, multi-functional, and modular self-reconfigurable robotic system. In *Proc. of IEEE/RSJ IROS*, pages 3636–3641, 2006.

[Stallings, 1997] W. Stallings. *Data and computer communications (5th ed.)*. Prentice-Hall, Inc., Upper Saddle River, NJ, USA, 1997.

[Yim *et al.*, 2000] M. Yim, D. Duff, and K. Roufas. Polybot: a modular reconfigurable robot. In *Proc. of IEEE ICRA*, pages 514–520, 2000.

[Yim *et al.*, 2007a] M. Yim, W.-M. Shen, B. Salemi, D. Rus, M. Moll, H. Lipson, E. Klavins, and G. Chirikjian. Modular self-reconfigurable robot systems: Challenges and opportunities for the future. *IEEE Robot. Automat. Mag.*, 14(1):43–52, March 2007.

[Yim *et al.*, 2007b] M. Yim, B. Shirmohammadi, J. Sastra, M. Park, M. Dugan, and C. Taylor. Towards robotic self-reassembly after explosion. In *Proc. of IEEE/RSJ IROS*, pages 2767–2772, 2007.